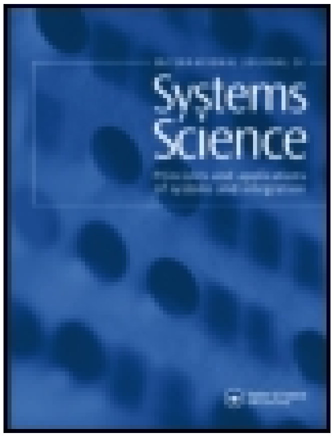

International Journal of Systems Science
Publication details, including instructions for authors and subscription information:
http://www.tandfonline.com/loi/tsys20

Robust adaptive tracking control of MIMO nonlinear systems in the presence of actuator hysteresis

Guiyuan Fu[a], Linlin Ou[b] & Weidong Zhang[a]

[a] Department of Automation, Shanghai Jiaotong University, and Key Laboratory of System Control and Information Processing, Ministry of Education of China, Shanghai, P R China

[b] Department of Automation, Zhejiang University of Technology, Hangzhou, P R China

Published online: 06 Jan 2015.

International Journal of Systems Science, 2014
http://dx.doi.org/10.1080/00207721.2014.994051

Robust adaptive tracking control of MIMO nonlinear systems in the presence of actuator hysteresis

Guiyuan Fu[a], Linlin Ou[b] and Weidong Zhang[a,*]

[a]*Department of Automation, Shanghai Jiaotong University, and Key Laboratory of System Control and Information Processing, Ministry of Education of China, Shanghai, P R China;* [b]*Department of Automation, Zhejiang University of Technology, Hangzhou, P R China*

(*Received 1 August 2014; accepted 28 November 2014*)

Adaptive tracking control of a class of MIMO nonlinear system preceded by unknown hysteresis is investigated. Based on dynamic surface control, an adaptive robust control law is developed and compensators are designed to mitigate the influences of both the unknown bounded external uncertainties and the unknown Prandtl–Islinskii hysteresis. By adopting the low-pass filters, the explosion of complexity caused by tedious computation of the time derivatives of the virtual control laws is overcome. With the proposed control scheme, the closed-loop system is proved to be semi-globally ultimately bounded by the Lyapunov stability theory, and the output of the controlled system can track the desired trajectories with an arbitrarily small error. Finally, numerical simulations are given to verify the effectiveness of the proposed approach.

Keywords: nonlinear MIMO system; Prandtl–Islinskii hysteresis; dynamic surface control; adaptive control

1. Introduction

Hysteresis exists in a wide range of physical systems and smart materials, e.g. tribology, electromagnetism, piezoelectrics, shape memory alloys, pneumatic artificial muscles and ionic polymer metal composites (Deng & Wang, 2012; Esbrook, Tan, & Khalil, 2013; Tan & Baras, 2004; Vo-Minh, Tjahjowidodoand, Ramon, & Van Brussel, 2011). The presence of hysteresis in the nonlinear systems often limits system performance and even causes instability (Tao & Kokotovic, 1995). However, hysteretic nonlinearities are generally complicated with multi-values and non-smooth features, which make the hysteretic control problem usually difficult and challenging. Owing to the growing industrial demands involving various applications of smart-material-based actuators and sensors, it has received increasing attention recently. Many mathematical models have been developed to characterise the behaviour of hysteresis, such as Presiach model, Prandtl–Ishlinskii (P-I) model, Duhem model, backlash hysteresis model, B-W model, etc. and interested readers can refer to Macki, Nistri and Zecca (1993). Meanwhile, various control methods have been put forward to control hysteresis in systems.

Generally, the research addressing hysteresis in control system can be classified into two groups. One is to construct the inversion of the hysteresis to compensate for the hysteretic effect (for example Esbrook et al. 2013; Gu, Zhu, & Su, 2014; Krejci & Kuhnen, 2001; Shan & Leang, 2009; Tan & Baras, 2004; Zhou, Wen, & Li, 2012). Nevertheless, constructing the inverse operator for the hysteresis model is always challenging; furthermore, this method is often complicated, computationally costly and possesses strong sensitivity of the model parameters to the unknown measurement errors. These issues are directly linked to the difficulties of guaranteeing the stability of systems except for certain special cases (Tao & Kokotovic, 1995). While the other is to develop the control algorithm without constructing the inverse model of the hysteresis (for example Cai, Wen, Su, & Liu, 2013; Li, Tong, & Li, 2012; Mousavi, Ranjbar-Sahraei, & Noroozi, 2012; Ren, San, Ge, & Lee, 2009; Su, Wang, Chen, & Rakheja, 2005), which has drawn much interest from control community, since it can allow designers to fuse the available robust control techniques to mitigate the effects of hysteresis. For example, based on dynamics surface control and neural network, Ren et al. (2009) proposed an adaptive robust control scheme for a class of uncertain strict feedback nonlinear system with backlash-like hysteresis, so that the output of the controlled system can track the desired trajectory with small error, where the backlash hysteresis is treated as a bounded disturbance-like term of the controlled system. Similarly, Cai et al. (2013) developed a backstepping-based adaptive robust controller for a class of the uncertain system with actuator with backlash-like hysteresis. Su et al. (2005) and Zhang, Lin, and Mao (2011) investigated adaptive robust control for a class of the nonlinear system with unknown P-I hysteresis, and variable structure control based controller and dynamic surface control (DSC) based controller

*Corresponding author. Email: wdzhang@sjtu.edu.cn

were developed, respectively, since the nonlinear item of P-I hysteresis cannot be assumed to be bounded as the backlash-like hysteresis, it is mitigated by designing another compensator.

While a large number of literatures are available on the robust control for uncertain SISO systems with unknown hysteresis, the number on MIMO systems with hysteresis is relatively small (Li et al., 2012; Mousavi et al., 2012; Parlangeli & Corradini, 2005). It is undoubtedly that MIMO system widely exists in the real world, e.g. aircraft (Tang, Tao, & Joshi 2007), robot (Qiao, Dai, Liu, & Wang, 2007) and HVAC system (Anderson et al. 2008). The adaptive control of MIMO systems has been extensively studied in the past decades from many aspects. For example, effective control strategies have been provided for the uncertain MIMO system with time-delays, dead-zones and input saturation constraints (Chen, Ge, & Ee, 2010; Zhang & Ge, 2007) and so on. Moreover, due to the increasing applications of smart-material-based actuators (for example Jain, Majumder, & Dutta, 2012; Kim et al., 2003; Shan & Leang, 2009), which inherently exhibit hysteretic nonlinearity, it is of great value and interest to study the nonlinear MIMO systems with hysteretic actuators. In this paper, robust adaptive tracking control of uncertain MIMO nonlinear system with unknown P-I hysteresis is investigated. The control goal is that the tracking error would be within an arbitrarily small set. To this end, a robust adaptive controller is developed based on DSC (Swaroop, Hedrick, Yip, & Gerdes, 2000), and compensator is designed to attenuate the effect of the external uncertainties. Since P-I hysteresis model contains an integral function, which is not assumed to be bounded, it cannot be simply treated as a bounded external disturbance-like term of the controlled system as in the literatures (Li et al. 2012; Mousavi et al., 2012; Parlangeli & Corradini, 2005). This would make the problem much more difficult, and in this paper, we introduce another compensator to compensate for the influence of the uncertain P-I hysteresis.

The main advantages of this paper are as follows: (1) by designing compensator, the proposed control scheme can mitigate the influences of both the unknown bounded external uncertainties and the P-I hysteresis which cannot be treated as a bounded disturbance-like term of the controlled system, and can be applied to a larger number of the system with hysteresis, (2) the information on the boundaries of external uncertainties is not needed and (3) the explosion of the complexity of traditional backstepping method is overcome by introducing the low-pass filter.

The rest of this paper is organised as follows. The description of P-I hysteresis and the problem formulation are given in Section 2. Section 3 presents the adaptive robust controller design and the theoretical analysis, while the simulation results are provided in Section 4. Finally, some conclusions are presented in Section 5.

2. Problem formulation and preliminaries

2.1. *Prandtl–Islinskii hysteresis*

As the sub-class of Presiach hysteresis model, P-I hysteresis is symmetric and rate independent and has been applied to describe the hysteretic behaviour of such smart-material-based actuator as PZT (Shan & Leang, 2009).

P-I hysteresis is an operator-type model and formulated through a weighted superposition of the so-called play operator or stop operator with threshold. The detail information can be found in Brokate and Sprekels (1996) and Shan and Leang (2009).

Let the input signal $u(t)$ is piecewise monotonous over the interval $(t_i, t_{i+1}]$ for $0 \le i \le N-1$ and $0 = t_0 < t_1 < \cdots < t_N$. Herein, by referring to Brokate and Sprekels (1996), the play operator $F_r[u; w_{-1}]$ and the stop operator $E_r[u; w_{-1}]$ with threshold r are defined as

$$\begin{aligned} F_r[u; w_{-1}](0) &= f_r(u(0), w_{-1}), \\ F_r[u; w_{-1}](t) &= f_r(u(t), F_r[u; w_{-1}](t_i)), \\ E_r[u; w_{-1}](0) &= e_r(u(0) - w_{-1}), \\ E_r[u; w_{-1}](t) &= e_r(u(t) - u(t_i) + E_r[u; w_{-1}](t_i)), \end{aligned}$$

where w_{-1} is the initial value before the input signal $u(t)$ is applied at time $t = 0$, and the function $f_r(u, \alpha) = \max(u - r, \min(u + r, \alpha))$ and $e_r(u) = \min(r, \max(-r, u))$.

It can be proved that the play operator $F_r[u; w_{-1}]$ is the complement of the stop operator $E_r[u; w_{-1}]$, i.e. $E_r[u; w_{-1}](t) + F_r[u; w_{-1}](t) = u(t)$.

P-I model can be defined by stop operator or play operator, both of which are equivalent. Here, we adopt the play operator to define P-I hysteresis, which can be expressed by Equation (1) by referring to Su et al. (2005) and Brokate and Sprekels (1996)

$$w(t) = u(t) \int_0^{\infty} p(r)\,dr - \int_0^{\infty} p(r) F_r[u](t)\,dr, \tag{1}$$

where $p(r)$ is the unknown density function, satisfying $p(r) \ge 0$ with $\int_0^{\infty} r p(r)\,dr < \infty$, and can affect the shape and size of the hysteresis curve.

Since the density function $p(r)$ vanishes for large value of r, it is reasonable to assume that there exists large enough constant R such that $p(r) = 0$ for $r > R$, although $R = \infty$ is commonly chosen as the upper limit of the integration. Denote the constant $p_0 = \int_0^R p(r)\,dr$, and Equation (1) can be expressed as

$$w(t) = p_0 u(t) - \int_0^{R} p(r) F_r[u](t)\,dr. \tag{2}$$

As an example, hysteresis curve generated from P-I model (2) is shown in Figure 1, where $p(r) = 0.5e^{-0.067(r-1)^2}$, with $r \in [0, 50]$, the input $u(t) = \frac{7 \sin 3t}{1+t}$

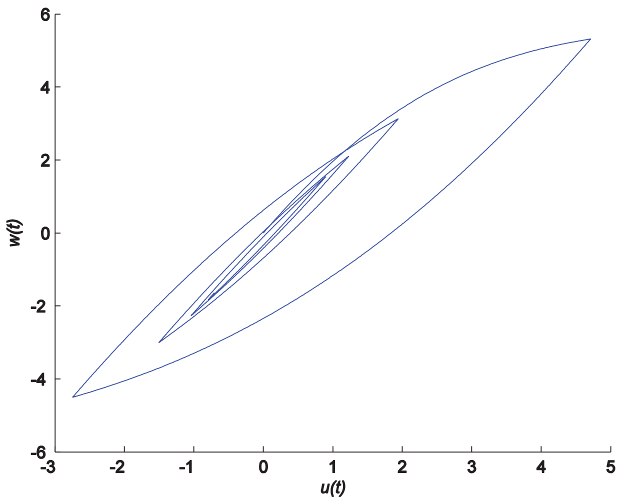

Figure 1. The illustration of P-I hysteresis.

with $t \in [0, 8]$, and w_{-1}, respectively. It can be indicated from Figure 1 that Equation (2) exhibits hysteresis indeed and can be taken to describe hysteretic behaviour.

2.2. Problem formulation

Consider the following MIMO model:

$$\begin{aligned}
\dot{\mathbf{x}}_1 &= \mathbf{F}_1(\bar{\mathbf{x}}_1, t)\boldsymbol{\theta}_1 + \mathbf{G}_1(\bar{\mathbf{x}}_1, t)\mathbf{x}_2 + \mathbf{D}_1(\bar{\mathbf{x}}_1, t),\\
&\vdots\\
\dot{\mathbf{x}}_{n-1} &= \mathbf{F}_{n-1}(\bar{\mathbf{x}}_{n-1}, t)\boldsymbol{\theta}_{n-1} + \mathbf{G}_{n-1}(\bar{\mathbf{x}}_{n-1}, t)\mathbf{x}_n\\
&\quad + \mathbf{D}_{n-1}(\bar{\mathbf{x}}_{n-1}, t),\\
\dot{\mathbf{x}}_n &= \mathbf{F}_n(\bar{\mathbf{x}}_n, t)\boldsymbol{\theta}_n + \mathbf{G}_n(\bar{\mathbf{x}}_n, t)\mathbf{w}(t) + \mathbf{D}_n(\bar{\mathbf{x}}_n, t),\\
\mathbf{y} &= \mathbf{x}_1,
\end{aligned} \tag{3}$$

where $\mathbf{x}_i \in R^m, i = 1, 2, \ldots, n$ are the state vectors and $\bar{\mathbf{x}}_i = [\mathbf{x}_1, \mathbf{x}_2, \ldots, \mathbf{x}_i]$; $\mathbf{F}_i \in R^{m\times q_i}$ are the known nonlinear system functions; $\boldsymbol{\theta}_i \in R^{q_i}$ are the uncertain system parameter vectors; $\mathbf{G}_i \in R^{m\times m}$ are the known invertible smooth control coefficient matrices; $\mathbf{D}_i \in R^m$ are the bounded unknown uncertainties; $\mathbf{y} \in R^m$ is the output of the system; while $\mathbf{w}(t) \in R^m = [w_1, \ldots, w_m]^T$ is the actual input of the controlled system and the output of the actuators with P-I hysteresis, where $w_i(t)(i = 1, 2, \ldots, m)$ is defined by Equation (2).

Without loss of generality, in this paper, we assume all the elements in $\mathbf{w}(t) = [w_1, \ldots, w_m]^T$ exhibit the same hysteretic behaviour in this work, i.e. $w_i(i = 1, 2, \ldots, m)$ have the same density function $p(r)$ and upper bound R, thus

$$w_i(t) = p_0 u_i(t) - \int_0^R p(r)F_r[u_i](t)\,dr, \quad (i = 1, \ldots, m). \tag{4}$$

Thus, Equation (4) can be rewritten in the form of vector

$$\mathbf{w}(t) = H[\mathbf{u}](t) = p_0\mathbf{u}(t) - \int_0^R p(r)F_r[\mathbf{u}](t)\,dr, \tag{5}$$

where $\mathbf{u} \in R^m = [u_1, \ldots, u_m]^T$.

Denote $H_N[\mathbf{u}](t) = [H_N[u_1], H_N[u_2], \ldots, H_N[u_m]]^T = \int_0^R p(r)F_r[\mathbf{u}]dr$, and by substituting Equation (5) into Equation (3), we have

$$\begin{aligned}
\dot{\mathbf{x}}_1 &= \mathbf{F}_1(\bar{\mathbf{x}}_1, t)\boldsymbol{\theta}_1 + \mathbf{G}_1(\bar{\mathbf{x}}_1, t)\mathbf{x}_2 + \mathbf{D}_1(\bar{\mathbf{x}}_1, t),\\
&\vdots\\
\dot{\mathbf{x}}_{n-1} &= \mathbf{F}_{n-1}(\bar{\mathbf{x}}_{n-1}, t)\boldsymbol{\theta}_{n-1} + \mathbf{G}_{n-1}(\bar{\mathbf{x}}_{n-1}, t)\mathbf{x}_n\\
&\quad + \mathbf{D}_{n-1}(\bar{\mathbf{x}}_{n-1}, t),\\
\dot{\mathbf{x}}_n &= \mathbf{F}_n(\bar{\mathbf{x}}_n, t)\boldsymbol{\theta}_n + p_0\mathbf{G}_n(\bar{\mathbf{x}}_n, t)\mathbf{u}(t) - \mathbf{G}_n(\bar{\mathbf{x}}_n, t)H_N[\mathbf{u}](t)\\
&\quad + \mathbf{D}_n(\bar{\mathbf{x}}_n, t),\\
\mathbf{y} &= \mathbf{x}_1.
\end{aligned} \tag{6}$$

The control objective is to design adaptive controller $\mathbf{u}(t)$ for system (6), such that the system output $\mathbf{y}$ can track the desired trajectories $\mathbf{y}_d$ in a small neighbourhood of zero in the presence of the system uncertainties and hysteretic nonlinearities, i.e. $\lim_{t\to\infty}\|\mathbf{y}(t) - \mathbf{y}_d(t)\| = \sigma$, where $\sigma \to 0$.

Remark 1: The nonlinear system expressed by (3) can present many practical systems such as aircraft (Tang et al., 2007), robot (Dawson, Carroll, & Schneider, 1994) and so on.

To facilitate the controller design, the following assumptions are made and some useful lemmas are presented.

Assumption 1: *For the unknown uncertainties and disturbances* $\mathbf{D}_i = [D_{i1}, \ldots, D_{im}]^T$, *there exists unknown bounded constants* $\varphi_{ij} > 0$ *such that* $|D_{ij}| \le \varphi_{ij}$, $j = 1, 2, \ldots, m$, *and denote* $\boldsymbol{\Xi}_i = [\varphi_{i1}, \ldots, \varphi_{im}]^T$.

Assumption 2: *The desired trajectories* $\mathbf{y}_d = [y_{d1}, \ldots, y_{dm}]^T$ *are continuous and available, and for every element in* $\mathbf{y}_d$, $[y_{di}, \dot{y}_{di}, \ddot{y}_{di}]^T \in \Omega_{di}$ $(i = 1, 2, \ldots, m)$, *with the known compact set* $\Omega_{di} = \{[y_{di}, \dot{y}_{di}, \ddot{y}_{di}]^T : y_{di}^2 + \dot{y}_{di}^2 + \ddot{y}_{di}^2 \le K_{0i}\}$.

Remark 2: Assumption 1 assumes that the disturbances are bounded, which is reasonable in practical engineering and have been claimed in other literatures (for example Ren et al., 2009; Li, Tong, & Li, 2012; Chen et al., 2010), while Assumption 2 is one of the basic requirements of DSC (Swaroop et al. 2000).

Lemma 1 (Polycarpou and Ioannou, 1996)**:** *The following inequality holds for any* $\varepsilon > 0$ *and for any* $\eta \in R$,

$$0 \le |\eta| - \eta\tanh\left(\frac{\eta}{\varepsilon}\right) \le k_p\varepsilon, \tag{7}$$

where k_p is a constant that satisfies $k_p = e^{-(k_p+1)}$, i.e. $k_p =$ 0.2758.

3. Main results

3.1. Adaptive controller design

In this section, the controller $\mathbf{u}(t)$ for the system (1) would be developed based on the adaptive DSC, which is based on the change of coordinates: $\mathbf{S}_1 = \mathbf{x}_1 - \mathbf{y}_d$, $\mathbf{S}_i = \mathbf{x}_i - \mathbf{x}_{id} (i = 2, 3, \ldots, n)$, where $\mathbf{S}_i \in R^m (i = 1, \ldots, n) = [S_{i1}, \ldots, S_{im}]^T$ is the error surface and $\mathbf{x}_{id}$ is the output of filtered virtual control signal $\underline{\mathbf{x}}_i (i = 2, \ldots, n) \in R^m$, which will be determined later. Before proceeding with the controller developing procedure, another error signals are defined as $\mathbf{z}_i = \mathbf{x}_{id} - \underline{\mathbf{x}}_i (i = 2, 3, \ldots, n)$, thus $\mathbf{x}_i = \mathbf{S}_i + \underline{\mathbf{x}}_i + \mathbf{z}_i$.

The controller design will be done in the following steps.

Step 1: for the first error surface $\mathbf{S}_1 = \mathbf{x}_1 - \mathbf{y}_d$, its derivative with respect to t along (6) is

$$\begin{aligned}\dot{\mathbf{S}}_1 &= \dot{\mathbf{x}}_1 - \dot{\mathbf{y}}_d = \mathbf{F}_1(\bar{\mathbf{x}}_1, t)\boldsymbol{\theta}_1 + \mathbf{G}_1(\bar{\mathbf{x}}_1, t)\mathbf{x}_2 + \mathbf{D}_1(\bar{\mathbf{x}}_1, t) - \dot{\mathbf{y}}_d \\ &= \mathbf{F}_1(\bar{\mathbf{x}}_1, t)\boldsymbol{\theta}_1 + \mathbf{G}_1(\bar{\mathbf{x}}_1, t)(\mathbf{S}_2 + \underline{\mathbf{x}}_2 + \mathbf{z}_2) \\ &\quad + \mathbf{D}_1(\bar{\mathbf{x}}_1, t) - \dot{\mathbf{y}}_d. \end{aligned} \tag{8}$$

Choose the Lyapunov candidate function as

$$V_1 = \frac{1}{2}\mathbf{S}_1^T\mathbf{S}_1 + \frac{1}{2}\tilde{\boldsymbol{\theta}}_1^{\mathbf{T}}\tilde{\boldsymbol{\theta}}_1 + \frac{1}{2}\tilde{\boldsymbol{\Xi}}_1^{\mathbf{T}}\tilde{\boldsymbol{\Xi}}_1 + \frac{1}{2}\mathbf{z}_2^T\mathbf{z}_2, \tag{9}$$

where $\tilde{\boldsymbol{\theta}}_1 = \boldsymbol{\theta}_1 - \hat{\boldsymbol{\theta}}_1$, $\tilde{\boldsymbol{\Xi}}_1 = \boldsymbol{\Xi}_1 - \hat{\boldsymbol{\Xi}}_1$ with $\hat{\boldsymbol{\theta}}_1$ and $\hat{\boldsymbol{\Xi}}_1$ as the estimations of the unknown system parameter vector $\boldsymbol{\theta}_1$ and unknown bounded constant vector $\boldsymbol{\Xi}_1$, respectively.

The derivative of (9) along system (6) is

$$\begin{aligned}\dot{V}_1 &= \mathbf{S}_1^T(\mathbf{F}_1(\bar{\mathbf{x}}_1, t)\boldsymbol{\theta}_1 + \mathbf{G}_1(\bar{\mathbf{x}}_1, t)(\mathbf{S}_2 + \underline{\mathbf{x}}_2 + \mathbf{z}_2) \\ &\quad + \mathbf{D}_1(\bar{\mathbf{x}}_1, t) - \dot{\mathbf{y}}_d) + +\tilde{\theta}_1^{\mathbf{T}}\dot{\tilde{\boldsymbol{\theta}}}_1 + \tilde{\boldsymbol{\Xi}}_1^{\mathbf{T}}\dot{\tilde{\boldsymbol{\Xi}}}_1 + \mathbf{z}_2^T\dot{\mathbf{z}}_2 \\ &\le \mathbf{S}_1^T\mathbf{F}_1(\bar{\mathbf{x}}_1, t)\boldsymbol{\theta}_1 + \mathbf{S}_1^T\mathbf{G}_1(\bar{\mathbf{x}}_1, t)\underline{\mathbf{x}}_2 + \mathbf{S}_1^T\mathbf{G}_1(\bar{\mathbf{x}}_1, t)(\mathbf{S}_2 + \mathbf{z}_2) \\ &\quad + \sum_{j=1}^{m}|S_{1j}||D_{1j}| - \mathbf{S}_1^T\dot{\mathbf{y}}_d + \tilde{\theta}_1^{\mathbf{T}}\dot{\tilde{\boldsymbol{\theta}}}_1 + \tilde{\boldsymbol{\Xi}}_1^{\mathbf{T}}\dot{\tilde{\boldsymbol{\Xi}}}_1 + \mathbf{z}_2^T\dot{\mathbf{z}}_2 \\ &\le \mathbf{S}_1^T\mathbf{F}_1(\bar{\mathbf{x}}_1, t)\boldsymbol{\theta}_1 + \mathbf{S}_1^T\mathbf{G}_1(\bar{\mathbf{x}}_1, t)\underline{\mathbf{x}}_2 + \mathbf{S}_1^T\mathbf{G}_1(\bar{\mathbf{x}}_1, t)(\mathbf{S}_2 + \mathbf{z}_2) \\ &\quad + \sum_{j=1}^{m}|S_{1j}|\varphi_{1j} - \mathbf{S}_1^T\dot{\mathbf{y}}_d + \tilde{\boldsymbol{\theta}}_1^{\mathbf{T}}\dot{\tilde{\boldsymbol{\theta}}}_1 + \tilde{\boldsymbol{\Xi}}_1^{\mathbf{T}}\dot{\tilde{\boldsymbol{\Xi}}}_1 + \mathbf{z}_2^T\dot{\mathbf{z}}_2. \end{aligned} \tag{10}$$

According to Lemma 1, it can be obtained that

$$\begin{aligned}\sum_{j=1}^{m}|S_{1j}|\varphi_{1j} &\le \sum_{j=1}^{m}\left(k_p\varepsilon_{1j} + S_{1j}\tanh\left(\frac{S_{1j}}{\varepsilon_{1j}}\right)\right)\varphi_{1j} \\ &= \boldsymbol{\Gamma}_1^T\boldsymbol{\Xi}_1 + \mathbf{S}_1^T\mathrm{Tanh}(\mathbf{S}_1)\boldsymbol{\Xi}_1,\end{aligned}$$

where denote $\boldsymbol{\Gamma}_1 = [k_p\varepsilon_{11}, \ldots, k_p\varepsilon_{1m}]^T$ and $\mathrm{Tanh}(\mathbf{S}_1) = \mathrm{diag}(\tanh\frac{S_{11}}{\varepsilon_{11}}, \ldots, \tanh\frac{S_{1m}}{\varepsilon_{1m}})$.

Thus Equation (10) yields

$$\begin{aligned}\dot{V}_1 &\le \mathbf{S}_1^T\mathbf{F}_1(\bar{\mathbf{x}}_1, t)\boldsymbol{\theta}_1 + \mathbf{S}_1^T\mathbf{G}_1(\bar{\mathbf{x}}_1, t)\underline{\mathbf{x}}_2 \\ &\quad + \mathbf{S}_1^T\mathbf{G}_1(\bar{\mathbf{x}}_1, t)(\mathbf{S}_2 + \mathbf{z}_2) + \boldsymbol{\Gamma}_1^T\boldsymbol{\Xi}_1 \\ &\quad + \mathbf{S}_1^T\mathrm{Tanh}(\mathbf{S}_1)\boldsymbol{\Xi}_1 - \mathbf{S}_1^T\dot{\mathbf{y}}_d + \tilde{\boldsymbol{\theta}}_1^{\mathbf{T}}\dot{\tilde{\boldsymbol{\theta}}}_1 + \tilde{\boldsymbol{\Xi}}_1^{\mathbf{T}}\dot{\tilde{\boldsymbol{\Xi}}}_1 + \mathbf{z}_2^T\dot{\mathbf{z}}_2.\end{aligned} \tag{11}$$

Choose the virtual control law as

$$\underline{\mathbf{x}}_2 = \mathbf{G}_1^{-1}(-k_1\mathbf{S}_1 - \mathbf{F}_1(\bar{\mathbf{x}}_1, t)\hat{\boldsymbol{\theta}}_1 - \mathrm{Tanh}(\mathbf{S}_1)\hat{\boldsymbol{\Xi}}_1 + \dot{\mathbf{y}}_d), \tag{12}$$

where k_1 is a positive constant and would be determined later.

The update laws of the unknown parameters $\hat{\boldsymbol{\theta}}_1$ and $\hat{\boldsymbol{\Xi}}_1$ are chosen as

$$\dot{\hat{\boldsymbol{\theta}}}_1 = \mathbf{F}_1^T(\bar{\mathbf{x}}_1, t)\mathbf{S}_1 - \rho_1\hat{\boldsymbol{\theta}}_1, \; \dot{\hat{\boldsymbol{\Xi}}}_1 = \mathrm{Tanh}(\mathbf{S}_1)\mathbf{S}_1 - \lambda_1\hat{\boldsymbol{\Xi}}_1, \tag{13}$$

where $\rho_1\lambda_1$ are positive designed parameters.

By substituting (12) and (13) into (11), it yields

$$\begin{aligned}\dot{V}_1 &\le -k_1\mathbf{S}_1^T\mathbf{S}_1 + \boldsymbol{\Gamma}_1^T\boldsymbol{\Xi}_1 + \mathbf{S}_1^T\mathbf{G}_1(\bar{\mathbf{x}}_1, t)(\mathbf{S}_2 + \mathbf{z}_2) \\ &\quad + \mathbf{z}_2^T\dot{\mathbf{z}}_2 + \rho_1\tilde{\boldsymbol{\theta}}_1^T\hat{\boldsymbol{\theta}}_1 + \lambda_1\tilde{\boldsymbol{\Xi}}_1^T\hat{\boldsymbol{\Xi}}_1.\end{aligned} \tag{14}$$

Let the virtual control $\underline{\mathbf{x}}_2$ pass through a first-order filter

$$\tau_2\dot{\mathbf{x}}_{2d} + \mathbf{x}_{2d} = \underline{\mathbf{x}}_2, \quad \mathbf{x}_{2d}(0) = \underline{\mathbf{x}}_2(0), \tag{15}$$

where τ_2 is the designed constant which can be chosen arbitrarily small and would be determined later.

Remark 3: From (15), we have $\dot{\mathbf{x}}_{2d} = \frac{\underline{\mathbf{x}}_2 - \mathbf{x}_{2d}}{\tau_2}$, such that it can avoid solving the derivative of $\mathbf{x}_{2d}$, which is the source of the 'explosive terms' in the traditional backstepping method.

Step$i (2 \le i \le n-1)$: for the error $\mathbf{S}_i = \mathbf{x}_i - \mathbf{x}_{id}$, its derivative along the system (6) is

$$\begin{aligned}\dot{\mathbf{S}}_i &= \mathbf{F}_i(\bar{\mathbf{x}}_i, t)\boldsymbol{\theta}_i + \mathbf{G}_i(\bar{\mathbf{x}}_i, t)\mathbf{x}_{i+1} + \mathbf{D}_i(\bar{\mathbf{x}}_i, t) - \dot{\mathbf{x}}_{id} \\ &= \mathbf{F}_i(\bar{\mathbf{x}}_i, t)\boldsymbol{\theta}_i + \mathbf{G}_i(\bar{\mathbf{x}}_i, t)(\mathbf{S}_i + \underline{\mathbf{x}}_{i+1} + \mathbf{z}_{i+1}) \\ &\quad + \mathbf{D}_i(\bar{\mathbf{x}}_i, t) - \dot{\mathbf{x}}_{id}.\end{aligned} \tag{16}$$

Choose the Lyapunov function candidate as

$$V_i = \frac{1}{2}\mathbf{S}_i^T\mathbf{S}_i + \frac{1}{2}\tilde{\boldsymbol{\theta}}_i^{\mathbf{T}}\tilde{\boldsymbol{\theta}}_i + \frac{1}{2}\tilde{\boldsymbol{\Xi}}_i^{\mathbf{T}}\tilde{\boldsymbol{\Xi}}_i + \frac{1}{2}\mathbf{z}_i^T\mathbf{z}_i, \tag{17}$$

where $\tilde{\boldsymbol{\theta}}_i = \boldsymbol{\theta}_i - \hat{\boldsymbol{\theta}}_i$, $\tilde{\boldsymbol{\Xi}}_i = \boldsymbol{\Xi}_i - \hat{\boldsymbol{\Xi}}_i$ with $\hat{\boldsymbol{\theta}}_i$ and $\hat{\boldsymbol{\Xi}}_i$ as the estimations of $\boldsymbol{\theta}_i$ and $\boldsymbol{\Xi}_i$.

By substituting (16) and invoking Lemma 1, its derivative can be obtained as

$$\begin{aligned}\dot{V}_i \le\ & \mathbf{S}_i^T\mathbf{F}_i(\bar{\mathbf{x}}_i,t)\boldsymbol{\theta}_i + \mathbf{S}_i^T\mathbf{G}_i(\bar{\mathbf{x}}_i,t)(\mathbf{S}_i + \underline{\mathbf{x}}_{i+1} + \mathbf{z}_{i+1}) \\ & + \boldsymbol{\Gamma}_1^T\boldsymbol{\Xi}_1 + \mathbf{S}_1^T\mathrm{Tanh}(\mathbf{S}_1)\boldsymbol{\Xi}_1 - \mathbf{S}_i^T\dot{\mathbf{x}}_{id} \\ & + \tilde{\boldsymbol{\theta}}_i^{\mathbf{T}}\dot{\tilde{\boldsymbol{\theta}}}_i + \tilde{\boldsymbol{\Xi}}_i^{\mathbf{T}}\dot{\tilde{\boldsymbol{\Xi}}}_i + \mathbf{z}_i^T\dot{\mathbf{z}}_i. \end{aligned} \tag{18}$$

Similarly, choose the virtual control as

$$\underline{\mathbf{x}}_{i+1} = \mathbf{G}_i^{-1}(-k_i\mathbf{S}_i - \mathbf{F}_i(\bar{\mathbf{x}}_i,t)\hat{\boldsymbol{\theta}}_i - \mathrm{Tanh}(\mathbf{S}_i)\hat{\Xi}_i + \dot{\mathbf{x}}_{id}), \tag{19}$$

where $k_i > 0$.

Adaptive update laws are given by

$$\dot{\hat{\boldsymbol{\theta}}}_i = \mathbf{F}_i^T(\bar{\mathbf{x}}_i,t)\mathbf{S}_i - \rho_i\hat{\boldsymbol{\theta}}_i,\ \dot{\hat{\boldsymbol{\Xi}}}_i = \mathrm{Tanh}(\mathbf{S}_i)\mathbf{S}_i - \lambda_i\hat{\Xi}_i, \tag{20}$$

where $\rho_i\lambda_i$ are positive designed parameters.

Substituting (19) and (20) into (18) yields

$$\begin{aligned}\dot{V}_i \le\ & -k_i\mathbf{S}_i^T\mathbf{S}_i + \mathbf{S}_i^T\mathbf{G}_i(\bar{\mathbf{x}}_i,t)(\mathbf{S}_{i+1} + \mathbf{z}_{i+1}) + \boldsymbol{\Gamma}_i^T\boldsymbol{\Xi}_i \\ & + \mathbf{z}_{i+1}^T\dot{\mathbf{z}}_{i+1} + \rho_i\tilde{\boldsymbol{\theta}}_i^T\hat{\boldsymbol{\theta}}_i + \lambda_i\tilde{\boldsymbol{\Xi}}_i^T\hat{\boldsymbol{\Xi}}_i. \end{aligned} \tag{21}$$

Let the virtual control law $\underline{\mathbf{x}}_{i+1}$ pass through the low-pass filter

$$\tau_{i+1}\dot{\mathbf{x}}_{(i+1)d} + \mathbf{x}_{(i+1)d} = \underline{\mathbf{x}}_{i+1},\ \mathbf{x}_{(i+1)d}(0) = \underline{\mathbf{x}}_{i+1}(0), \tag{22}$$

where τ_{i+1} is a positive designed parameter that will be chosen later.

Step$n$: In this final step, the adaptive control law will be presented. The derivative of the final error surface $\mathbf{S}_n = \mathbf{x}_n - \mathbf{x}_{nd}$ along the system (6) is

$$\begin{aligned}\dot{\mathbf{S}}_n =\ & \dot{\mathbf{x}}_n - \dot{\mathbf{x}}_{nd} = \mathbf{F}_n(\bar{\mathbf{x}}_n,t)\boldsymbol{\theta}_n + p_0\mathbf{G}_n(\bar{\mathbf{x}}_n,t)\mathbf{u}(t) \\ & + \mathbf{D}_n(\bar{\mathbf{x}}_n,t) - \mathbf{G}_n(\bar{\mathbf{x}}_n,t)H_N[\mathbf{u}](t) - \dot{\mathbf{x}}_{nd}. \end{aligned} \tag{23}$$

Consider the following Lyapunov function candidate

$$V_{S_n} = \frac{1}{2}\mathbf{S}_n^T\mathbf{S}_n. \tag{24}$$

By differentiating (24) along (23) and invoking Lemma 1, it yields

$$\begin{aligned}\dot{V}_{S_n} \le\ & \mathbf{S}_n^T\mathbf{F}_n(\bar{\mathbf{x}}_n,t)\boldsymbol{\theta}_n + \mathbf{S}_n^Tp_0\mathbf{G}_n(\bar{\mathbf{x}}_n,t)\mathbf{u}(t) \\ & + \boldsymbol{\Gamma}_n^T\boldsymbol{\Xi}_n + \mathbf{S}_n^T\mathrm{Tanh}(\mathbf{S}_n)\boldsymbol{\Xi}_n \\ & - \mathbf{S}_n^T\mathbf{G}_n(\bar{\mathbf{x}}_n,t)H_N[\mathbf{u}](t) - \mathbf{S}_n^T\dot{\mathbf{x}}_{nd} \\ \le\ & \mathbf{S}_n^T\mathbf{F}_n(\bar{\mathbf{x}}_n,t)\boldsymbol{\theta}_n + \mathbf{S}_n^Tp_0\mathbf{G}_n(\bar{\mathbf{x}}_n,t)\mathbf{u}(t) + \boldsymbol{\Gamma}_n^T\boldsymbol{\Xi}_n \\ & + \mathbf{S}_n^T\mathrm{Tanh}(\mathbf{S}_n)\boldsymbol{\Xi}_n - \mathbf{S}_n^T\dot{\mathbf{x}}_{nd} \\ & + \|\mathbf{G}_n(\bar{\mathbf{x}}_n,t)\|\,\mathbf{S}_n^T Sgn(\mathbf{S}_n)\bar{H}_N[\mathbf{u}](t), \end{aligned} \tag{25}$$

where $Sgn(\mathbf{S}_n) = \mathrm{diag}(\mathrm{sgn}(S_{n1}), \mathrm{sgn}(S_{n2}), \ldots, \mathrm{sgn}(S_{nm}))$ and $\bar{H}_N[\mathbf{u}](t) = \int_0^R p(r)\bar{F}_r[\mathbf{u}]dr$ with $\bar{F}_r[\mathbf{u}] = [|F_r[u_1]|, \ldots, |F_r[u_m]|]^T$.

Remark 4: It should be noted that unlike the backlash-like hysteresis, whose nonlinearities can be regarded as bounded disturbance-like term, the nonlinear term $H_N[\mathbf{u}](t)$ in P-I hysteresis (5) cannot be assumed to be bounded, since $H_N[\mathbf{u}](t)$ is presented as an integral function of the unknown density function $p(r)$ and the play operator $F_r[\mathbf{u}]$, which may be unbounded with the input.

Remark 5: $\bar{H}(\mathbf{u})$ would be discretised by $\bar{H}[\mathbf{u}] = \sum_{i=0}^N \hat{p}(i\Delta r)\bar{F}_{i\Delta r}[\mathbf{u}]\Delta r$, where N is the level of discretisation such that $N = \frac{R}{\Delta r}$, and its size depends on the trade-off of the accuracy of discretisation and computation efficiency, and usually it is neither very small nor very large.

Choose the control law as

$$\mathbf{u} = \hat{\chi}\mathbf{u}_H, \tag{26}$$

$$\begin{aligned}\mathbf{u}_H =\ & \mathbf{G}_n^{-1}[-k_n(\mathbf{S}_n - \boldsymbol{\upsilon}) - \mathbf{F}_n(\bar{\mathbf{x}}_n,t)\hat{\boldsymbol{\theta}}_n - \mathrm{Tanh}(\mathbf{S}_n)\hat{\boldsymbol{\Xi}}_n \\ & + \mathbf{u}_{HC} + \dot{\mathbf{x}}_{nd}], \end{aligned} \tag{27}$$

$$\mathbf{u}_{HC} = -\|\mathbf{G}_n(\bar{\mathbf{x}}_n,t)\|Sgn(\mathbf{S}_n)\hat{\bar{H}}[\mathbf{u}](t), \tag{28}$$

where $k_n > 0$ is a small positive constant which will be chosen in accordance with the tracking performance, $\hat{\chi}$ is the estimation of $\frac{1}{p_0}$ and $\hat{\bar{H}}[\mathbf{u}] = \int_0^R \hat{p}(r)\bar{F}_r[\mathbf{u}]dr$, where $\hat{p}(r)$ is the estimation of the density function $p(r)$.

Remark 6: Since the density function $p(r)$ is not a function of time t, it can be treated as parameters of hysteresis model and estimated by an adaptive law.

The update laws of the parameters are chosen as

$$\begin{aligned} \dot{\hat{\boldsymbol{\theta}}}_n &= \mathbf{F}_n^T(\bar{\mathbf{x}}_n,t)\mathbf{S}_n - \rho_n\hat{\boldsymbol{\theta}}_n, \\ \dot{\hat{\boldsymbol{\Xi}}}_n &= \mathrm{Tanh}(\mathbf{S}_n)\mathbf{S}_n - \lambda_n\hat{\Xi}_n, \\ \dot{\hat{\chi}} &= -\mathbf{S}_n^T\mathbf{G}_n(\bar{\mathbf{x}}_n,t)\mathbf{u}_H - \sigma\hat{\chi}, \\ \frac{\partial\hat{p}(r)}{\partial t} &= \|\mathbf{G}_n\|\,\mathbf{S}_n^T Sgn(\mathbf{S}_n)\bar{F}_r(\mathbf{u}) - \kappa\hat{p}(r), \end{aligned} \tag{29}$$

where $\rho_n, \lambda_n, \sigma, \kappa$ are positive designed parameters.

Define the error signals $\tilde{\bar{H}}[\mathbf{u}] = \bar{H}[\mathbf{u}] - \hat{\bar{H}}[\mathbf{u}] = \int_0^R [p(r) - \hat{p}(r)]\bar{F}_r[\mathbf{u}]dr$, $\tilde{\boldsymbol{\theta}}_n = \boldsymbol{\theta}_n - \hat{\boldsymbol{\theta}}_n$, $\tilde{\boldsymbol{\Xi}}_n = \boldsymbol{\Xi}_n - \hat{\boldsymbol{\Xi}}_n$, $\tilde{\chi} = {}^1\!/_{p_0} - \hat{\chi}$ and consider the augmented Lyapunov function as

$$V_n = V_{S_n} + \frac{1}{2}\tilde{\boldsymbol{\theta}}_n^{\mathbf{T}}\tilde{\boldsymbol{\theta}}_n + \frac{1}{2}\tilde{\boldsymbol{\Xi}}_n^T\tilde{\boldsymbol{\Xi}}_n + \frac{p_0}{2}\tilde{\chi}^2 + \frac{1}{2}\int_0^R \tilde{p}(t,r)^2dr \tag{30}$$

By substituting (25)–(29), its derivative is obtained as

$$\dot{V}_n \leq -k_n \mathbf{S}_n^T \mathbf{S}_n + \boldsymbol{\Gamma}_n^T \boldsymbol{\Xi}_n + \rho_n \tilde{\boldsymbol{\theta}}_n^T \hat{\boldsymbol{\theta}}_n + \lambda_n \tilde{\boldsymbol{\Xi}}_n^T \hat{\boldsymbol{\Xi}}_n + p_0 \sigma \tilde{\chi} \hat{\chi} + \kappa \int_0^R \tilde{p}(t,r)\hat{p}(t,r)dr. \quad (31)$$

Remark 7: $\mathrm{Tanh}(\mathbf{S}_i)\hat{\boldsymbol{\Xi}}_i (i = 1, 2, \ldots, n)$ in (12), (19), (27) is introduced to compensate for the influence of the bounded disturbances $D_i (i = 1, 2, \ldots, n)$.

Remark 8: In (28), by estimating the value of $1/p_0$ rather than p_0, it can avoid the extreme situation that when $\hat{p}_0$ is zero, $1/\hat{p}_0$ will not exist.

Remark 9: The compensator $\mathbf{u}_{HC}$ in (27) is designed to mitigate the effect of P-I hysteresis.

Remark 10: It can be indicated that when such the bounded hysteresis as backlash hysteresis is considered in the controlled system, the proposed controller (27) is also applicable as long as we set the compensator $\mathbf{u}_{HC}$ as zero.

Now, we present the main result of this paper as follows:

Theorem 1: *For the uncertain MIMO system of* (6) *under Assumptions* 1–3 *and given that all the full information of states of* (6) *are available, if the proposed control law* (26), (27), (28) *and adaptive update laws* (13), (20), (29) *are employed, then with any bounded initial condition of the controlled system* (6), *the following results would be ensured:*

(1) all the signals of the closed-loop control system (6) are semi-globally ultimately uniformly bounded;
(2) the trajectories of the system output $\mathbf{y}(t)$ can asymptotically approach that of the desired $\mathbf{y}_d(t)$ with an arbitrarily small tracking error, i.e. $\lim_{t\to\infty} \|\mathbf{y}(t) - \mathbf{y}_d(t)\| = \sigma$ can be achieved.

3.2. Stability analysis

In this section, we will present the proof of Theorem 1 and analyse the stability of the system (6) under the proposed control scheme.

Proof: As for the filter error $\mathbf{z}_2 = \mathbf{x}_{2d} - \underline{\mathbf{x}}_2$, with $\mathbf{z}_2 = [z_{21}, \ldots, z_{2m}]^T$, we have its derivative by considering (12)

$$\dot{\mathbf{z}}_2 = \dot{\mathbf{x}}_{2d} - \dot{\underline{\mathbf{x}}}_2 = \dot{\mathbf{x}}_{2d} - \dot{\bar{\mathbf{G}}}_1(-k_1\mathbf{S}_1 - \mathbf{F}_1(\bar{\mathbf{x}}_1,t)\hat{\boldsymbol{\theta}}_1 - \mathrm{Tanh}(\mathbf{S}_1)\hat{\boldsymbol{\Xi}}_1 + \dot{\mathbf{y}}_d) - \bar{\mathbf{G}}_1\Big(-k_1\dot{\mathbf{S}}_1 - \mathbf{F}_1(\bar{\mathbf{x}}_1,t)\dot{\hat{\boldsymbol{\theta}}}_1 - \frac{\partial \mathbf{F}_1(\bar{\mathbf{x}}_1,t)}{\partial \bar{\mathbf{x}}_1^T}\hat{\boldsymbol{\theta}}_1 - \mathrm{Tanh}(\mathbf{S}_1)\dot{\hat{\boldsymbol{\Xi}}}_1 - (I_m - \mathrm{Tanh}(\mathbf{S}_1)\mathrm{Tanh}(\mathbf{S}_1))\hat{\boldsymbol{\Xi}}_1 + \ddot{\mathbf{y}}_d\Big). \quad (32)$$

Since $\dot{\mathbf{x}}_{2d} = \frac{\mathbf{x}_2 - \mathbf{x}_{2d}}{\tau_2} = -\frac{\mathbf{z}_2}{\tau_2}$, (32) can be rewritten as

$$\dot{\mathbf{z}}_2 + \frac{\mathbf{z}_2}{\tau_2} = -\dot{\bar{\mathbf{G}}}_1[-k_1\mathbf{S}_1 - \mathbf{F}_1(\bar{\mathbf{x}}_1,t)\hat{\boldsymbol{\theta}}_1 - \mathrm{Tanh}(\mathbf{S}_1)\hat{\boldsymbol{\Xi}}_1 + \dot{\mathbf{y}}_d] - \bar{\mathbf{G}}_1\Big[-k_1\dot{\mathbf{S}}_1 - \mathbf{F}_1(\bar{\mathbf{x}}_1,t)\dot{\hat{\boldsymbol{\theta}}}_1 - \frac{\partial \mathbf{F}_1(\bar{\mathbf{x}}_1,t)}{\partial \bar{\mathbf{x}}_1^T}\hat{\boldsymbol{\theta}}_1 - \mathrm{Tanh}(\mathbf{S}_1)\dot{\hat{\boldsymbol{\Xi}}}_1 - [I_m - \mathrm{Tanh}(\mathbf{S}_1)^2]\hat{\boldsymbol{\Xi}}_1 + \ddot{\mathbf{y}}_d\Big]. \quad (33)$$

As such

$$\left|\dot{z}_{2j} + \frac{z_{2j}}{\tau_2}\right| \leq \eta_{2j}(\mathbf{S}_1, \mathbf{S}_2, k_1, \mathbf{z}_2, \hat{\boldsymbol{\theta}}_1, \hat{\boldsymbol{\Xi}}_1, \mathbf{y}_d, \dot{\mathbf{y}}_d, \ddot{\mathbf{y}}_d), \quad j = 1, 2, \ldots, m, \quad (34)$$

where $\eta_{2j}(\mathbf{S}_1, \mathbf{S}_2, k_1, \mathbf{z}_2, \hat{\boldsymbol{\theta}}_1, \hat{\boldsymbol{\Xi}}_1, \mathbf{y}_d, \dot{\mathbf{y}}_d, \ddot{\mathbf{y}}_d)$ is a continuous function. Thus, we can have

$$\mathbf{z}_2^T \dot{\mathbf{z}}_2 \leq -\frac{\mathbf{z}_2^T \mathbf{z}_2}{\tau_2} + \sum_{i=1}^m |z_{2i}|\, \eta_{2i}. \quad (35)$$

By induction,

$$\dot{\mathbf{z}}_{i+1} + \frac{\mathbf{z}_{i+1}}{\tau_{i+1}} = -\dot{\bar{\mathbf{G}}}_i[-k_i\mathbf{S}_i - \mathbf{F}_i(\bar{\mathbf{x}}_i,t)\hat{\boldsymbol{\theta}}_i - \mathrm{Tanh}(\mathbf{S}_i)\hat{\boldsymbol{\Xi}}_i + \dot{\mathbf{x}}_{id}] - \bar{\mathbf{G}}_i\Big[-k_i\dot{\mathbf{S}}_i - \mathbf{F}_i(\bar{\mathbf{x}}_i,t)\dot{\hat{\boldsymbol{\theta}}}_i - \frac{\partial \mathbf{F}_i(\bar{\mathbf{x}}_i,t)}{\partial \bar{\mathbf{x}}_i^T}\dot{\bar{\mathbf{x}}}_i\hat{\boldsymbol{\theta}}_i - \mathrm{Tanh}(\mathbf{S}_i)\dot{\hat{\boldsymbol{\Xi}}}_i - [I_m - \mathrm{Tanh}(\mathbf{S}_i)^2]\hat{\boldsymbol{\Xi}}_i + \ddot{\mathbf{x}}_{id}\Big], \quad (36)$$

where $i = 2, \ldots, n-1$. As such

$$\left|\dot{z}_{(i+1)j} + \frac{z_{(i+1)j}}{\tau_{(i+1)}}\right| \leq \eta_{(i+1)j}(\mathbf{S}_1, \ldots, \mathbf{S}_{i+1}, k_1, \ldots, k_i, \mathbf{z}_2, \ldots, \mathbf{z}_{i+1}, \hat{\boldsymbol{\theta}}_i, \hat{\boldsymbol{\Xi}}_i, \mathbf{y}_d, \dot{\mathbf{y}}_d, \ddot{\mathbf{y}}_d), \quad (37)$$

where $j = 1, 2, \ldots, m$, and $\eta_{(i+1)j}(\mathbf{S}_1, \ldots, \mathbf{S}_{i+1}, k_1, \ldots, k_i, \mathbf{z}_2, \ldots, \mathbf{z}_{i+1}, \hat{\boldsymbol{\theta}}_i, \hat{\boldsymbol{\Xi}}_i, \mathbf{y}_d, \dot{\mathbf{y}}_d, \ddot{\mathbf{y}}_d)$ is a continuous function. Thus

$$\mathbf{z}_{i+1}^T \dot{\mathbf{z}}_{i+1} \leq -\frac{\mathbf{z}_{i+1}^T \mathbf{z}_{i+1}}{\tau_{i+1}} + \sum_{j=1}^m |z_{(i+1)j}|\eta_{(i+1)j}. \quad (38)$$

By substituting (38) into (14) and according to Young's equality, it can be represented as

$$\begin{aligned}\dot{V}_1 \le& -k_1\mathbf{S}_1^T\mathbf{S}_1 + \mathbf{\Gamma}_1^T\mathbf{\Xi}_1 + \mathbf{S}_1^T\mathbf{G_1}(\bar{\mathbf{x}}_1,t)(\mathbf{S}_2+\mathbf{z}_2)\\ &-\frac{\mathbf{z}_2^T\mathbf{z}_2}{\tau_2} + \sum_{i=1}^m |z_{2i}|\eta_{2i} + \rho_1\tilde{\boldsymbol{\theta}}_1^T\hat{\boldsymbol{\theta}}_1 + \lambda_1\tilde{\mathbf{\Xi}}_1^T\hat{\mathbf{\Xi}}_1\\ \le& (-k_1 + \|\mathbf{G_1}(\bar{\mathbf{x}}_1,t)\|^2)\mathbf{S}_1^T\mathbf{S}_1 + \frac{1}{2}\|\mathbf{S}_2\|^2 + \frac{1}{2}\|\mathbf{z}_2\|^2\\ &+\frac{1}{2}\|\mathbf{\Gamma}_1\|^2 + \frac{1}{2}\|\mathbf{\Xi}_1\|^2\\ &-\frac{\mathbf{z}_2^T\mathbf{z}_2}{\tau_2} + \sum_{j=1}^m |z_{2j}|\eta_{2j} + \rho_1\tilde{\boldsymbol{\theta}}_1^T\hat{\boldsymbol{\theta}}_1 + \lambda_1\tilde{\mathbf{\Xi}}_1^T\hat{\mathbf{\Xi}}_1. \end{aligned} \tag{39}$$

Similarly, (21) can be represented as

$$\begin{aligned}\dot{V}_i \le& -k_i\mathbf{S}_i^T\mathbf{S}_i + \mathbf{S}_i^T\mathbf{G}_i(\bar{\mathbf{x}}_i,t)(\mathbf{S}_{i+1}+\mathbf{z}_{i+1}) + \mathbf{\Gamma}_i^T\mathbf{\Xi}_i\\ &-\frac{\mathbf{z}_{i+1}^T\mathbf{z}_{i+1}}{\tau_{i+1}} + \sum_{j=1}^m |z_{(i+1)j}|\eta_{(i+1)j}\\ &+\rho_i\tilde{\boldsymbol{\theta}}_i^T\hat{\boldsymbol{\theta}}_i + \lambda_i\tilde{\mathbf{\Xi}}_i^T\hat{\mathbf{\Xi}}_i\\ \le& (-k_i + \|\mathbf{G}_i(\bar{\mathbf{x}}_i,t)\|^2)\mathbf{S}_i^T\mathbf{S}_i + \frac{1}{2}\|\mathbf{S}_{i+1}\|^2 + \frac{1}{2}\|\mathbf{z}_{i+1}\|^2\\ &+\frac{1}{2}\|\mathbf{\Gamma}_i\|^2 + \frac{1}{2}\|\mathbf{\Xi}_i\|^2\\ &-\frac{\mathbf{z}_{i+1}^T\mathbf{z}_{i+1}}{\tau_{i+1}} + \sum_{j=1}^m |z_{(i+1)j}|\eta_{(i+1)j} + \rho_i\tilde{\boldsymbol{\theta}}_i^T\hat{\boldsymbol{\theta}}_i + \lambda_i\tilde{\mathbf{\Xi}}_i^T\hat{\mathbf{\Xi}}_i. \end{aligned} \tag{40}$$

Consider the Lyapunov function of the controlled system (6):

$$V = \sum_{i=1}^n V_i. \tag{41}$$

Considering (31), (39), (40), we have its derivative as

$$\begin{aligned}\dot{V} \le& [-k_1 + \|\mathbf{G}_1(\bar{\mathbf{x}}_1,t)\|^2]\|\mathbf{S}_1\|^2\\ &+\sum_{i=2}^{n-1}\left[-k_i + \|\mathbf{G}_i(\bar{\mathbf{x}}_i,t)\|^2 + \frac{1}{2}\right]\|\mathbf{S}_i\|^2\\ &+\left(-k_n + \frac{1}{2}\right)\|\mathbf{S}_n\|^2 + \frac{1}{2}\sum_{i=1}^n\|\mathbf{\Gamma}_i\|^2 + \frac{1}{2}\sum_{i=1}^{i=n}\|\mathbf{\Xi}_i\|^2\\ &-\sum_{i=1}^{n-1}\frac{\mathbf{z}_{i+1}^T\mathbf{z}_{i+1}}{\tau_{i+1}} + \sum_{i=1}^{n-1}\sum_{j=1}^m |z_{(i+1)j}|\eta_{(i+1)j}\\ &+\sum_{i=1}^n\left(\rho_i\tilde{\boldsymbol{\theta}}_i^T\hat{\boldsymbol{\theta}}_i + \lambda_i\tilde{\mathbf{\Xi}}_i^T\hat{\mathbf{\Xi}}_i\right)\\ &+p_0\sigma\tilde{\chi}\hat{\chi} + \kappa\int_0^R \tilde{p}(t,r)\hat{p}(t,r)dr. \end{aligned} \tag{42}$$

Since for any $K_{0i} > 0$, the sets $\Omega_{di} = \{[y_{di}, \dot{y}_{di}, \ddot{y}_{di}]^T : y_{di}^2 + \dot{y}_{di}^2 + \ddot{y}_{di}^2 \le K_{0i}\}$ are compact in R^3. For any given $p > 0$, the sets $\Omega_k = \{\sum_{j=1}^k V_j \le 2p\}$, $k = 1, 2, \ldots, n$, are compact set. $\eta_{(i+1)j}(\cdot)$ has a maximum $M_{(i+1)j}$ on $\Omega_{di} \times \Omega_k$.

Invoking Young's inequality, we have

$$\begin{aligned}\sum_{j=1}^m |z_{(i+1)j}|\eta_{(i+1)j} \le& \sum_{j=1}^m |z_{(i+1)j}|M_{(i+1)j}\\ \le& \sum_{j=1}^m\left(\frac{z_{(i+1)j}^2 M_{(i+1)j}^2}{2\mu} + \frac{\mu}{2}\right). \end{aligned} \tag{43}$$

By denoting $M_{i+1} = \max\{M_{(i+1)1}, \ldots M_{(i+1)j}\ldots, M_{(i+1)m}\}$, (43) can be represented as

$$\begin{aligned}\sum_{j=1}^m |z_{(i+1)j}|\eta_{(i+1)j} \le& \sum_{j=1}^m\left(\frac{z_{(i+1)j}^2 M_{(i+1)j}^2}{2\mu} + \frac{\mu}{2}\right)\\ \le& \frac{M_{i+1}^2}{2\mu}\mathbf{z}_{i+1}^T\mathbf{z}_{i+1} + \frac{m\mu}{2}. \end{aligned} \tag{44}$$

By substituting (44) into (42), we have

$$\begin{aligned}\dot{V} \le& (-k_1 + \|\mathbf{G}_1(\bar{\mathbf{x}}_1,t)\|^2)\|\mathbf{S}_1\|^2\\ &+\sum_{i=2}^{n-1}\left[-k_i + \|\mathbf{G}_i(\bar{\mathbf{x}}_i,t)\|^2 + \frac{1}{2}\right]\|\mathbf{S}_i\|^2\\ &+\left(-k_n + \frac{1}{2}\right)\|\mathbf{S}_n\|^2\\ &+\frac{1}{2}\sum_{i=1}^n\|\mathbf{\Xi}_i\|^2 + \sum_{i=1}^{n-1}\left(\frac{M_{i+1}^2}{2\mu} - \frac{1}{\tau_{i+1}} + \frac{1}{2}\right)\|\mathbf{z}_{i+1}\|^2\\ &+\frac{m(n-1)\mu}{2} + \sum_{i=1}^n\left(\rho_i\tilde{\boldsymbol{\theta}}_i^T\hat{\boldsymbol{\theta}}_i + \lambda_i\tilde{\mathbf{\Xi}}_i^T\hat{\mathbf{\Xi}}_i\right)\\ &+p_0\sigma\tilde{\chi}\hat{\chi} + \kappa\int_0^R \tilde{p}(t,r)\hat{p}(t,r)dr. \end{aligned} \tag{45}$$

Invoking the Young's inequality, we have the following inequalities

$$\begin{aligned}&\tilde{\boldsymbol{\theta}}_i^T\hat{\boldsymbol{\theta}}_i = \tilde{\boldsymbol{\theta}}_i^T(\boldsymbol{\theta}_i - \tilde{\boldsymbol{\theta}}_i) \le \frac{1}{2}\|\boldsymbol{\theta}_i\|^2 - \frac{1}{2}\left\|\tilde{\boldsymbol{\theta}}_i\right\|^2,\\ &\tilde{\mathbf{\Xi}}_i^T\hat{\mathbf{\Xi}}_i = \tilde{\mathbf{\Xi}}_i^T(\mathbf{\Xi}_i - \tilde{\mathbf{\Xi}}_i) \le \frac{1}{2}\|\mathbf{\Xi}_i\|^2 - \frac{1}{2}\left\|\tilde{\mathbf{\Xi}}_i\right\|^2,\\ &\tilde{\chi}\hat{\chi} = \tilde{\chi}(\chi - \tilde{\chi}) \le \frac{1}{2}\chi^2 - \frac{1}{2}\tilde{\chi}^2,\\ &\int_0^R \tilde{p}(t,r)\hat{p}(t,r)dr = \int_0^R \tilde{p}(t,r)[p(t,r) - \tilde{p}(t,r)]dr\\ &\quad\le \int_0^R\left[\frac{1}{2}p(t,r)^2 - \frac{1}{2}\tilde{p}(t,r)^2\right]dr. \end{aligned} \tag{46}$$

Choose the designed parameters as

$$k_1 \geq \|\mathbf{G}_1(\bar{\mathbf{x}}_1, t)\|^2 + \alpha_0,$$
$$k_i \geq \|\mathbf{G}_i(\bar{\mathbf{x}}_i, t)\|^2 + \frac{1}{2} + \alpha_0, (i = 2, 3, \ldots, n-1),$$
$$k_n \geq \frac{3}{2} + \alpha_0,$$
$$\frac{1}{\tau_{i+1}} \geq \frac{M_{i+1}^2}{2\mu} + \frac{1}{2} + \alpha_0,$$
$$\rho_i \geq \alpha_0, \quad \lambda_i \geq \alpha_0, \quad i = 1, 2, \ldots, n,$$
$$\sigma \geq \alpha_0, \quad \kappa \geq \alpha_0, \quad k_{n1} > 1 + \alpha_0, \quad k_{n2} > \alpha_0, \qquad (47)$$

where α_0 is a positive constant.

By substituting (46) and (47) into (45), we can have

$$\dot{V} \leq -\alpha_0 V + C, \qquad (48)$$

where $C = \frac{1}{2}\sum_{i=1}^{n} \rho_i \|\boldsymbol{\theta}_i\|^2 + \frac{1}{2}\sum_{i=1}^{i=n}(1+\lambda_i)\|\boldsymbol{\Xi}_i\|^2 + \frac{p_0\sigma}{2}\chi^2 + \frac{1}{2}\int_0^R p(t,r)^2 dr + \frac{m(n-1)\mu}{2}$.

If $\alpha_0 > {}^{C}\!/_{p}$, it follows from (48) that $\dot{V} < 0$ on $V = p$; thus, $V \leq p$ is an invariant set, i.e. if $V(0) \leq p$, then $V(t) \leq p$ for all $t > 0$.

By integrating both sides of Equation (48), it can be solved by

$$0 \leq V(t) \leq \left[V(0) - \frac{C}{\alpha_0}\right] e^{-\alpha_0 t} + \frac{C}{\alpha_0}. \qquad (49)$$

Moreover, it can be obtained from (49) that

$$\lim_{t\to\infty} \|\mathbf{y}(t) - \mathbf{y}_d(t)\|^2 \leq \lim_{t\to\infty} V(t) = \frac{C}{\alpha_0}. \qquad (50)$$

It can be implied that V(t) is bounded, and all the signals of the closed-loop system, i.e. $\mathbf{S}_i, \tilde{\boldsymbol{\theta}}_i, \tilde{\boldsymbol{\Xi}}_i, z_{i+1}, \tilde{\chi}, \tilde{p}(r)$ are semi-globally uniformly bounded. Moreover, by adjusting the designed parameters, we can make $\frac{C}{\alpha_0}$ arbitrarily small, that is the tracking errors can be made within an arbitrarily small set. Usually, the larger α_0, the smaller tracking error. However, if α_0 is too large, so is the control gain of $\mathbf{u}$, i.e. the amplitude of the controller $\mathbf{u}$ would become very large. Thus, it should be balanced in the real world application.

4. Numerical Simulations

Consider the following two-order uncertain MIMO nonlinear system with unknown P-I hysteresis:

$$\dot{\mathbf{x}}_1 = \mathbf{F}_1(\bar{\mathbf{x}}_1, t)\boldsymbol{\theta}_1 + \mathbf{G}_1(\bar{\mathbf{x}}_1, t)\mathbf{x}_2 + \mathbf{D}_1(\bar{\mathbf{x}}_1, t),$$
$$\dot{\mathbf{x}}_2 = \mathbf{F}_2(\bar{\mathbf{x}}_2, t)\boldsymbol{\theta}_2 + \mathbf{G}_2(\bar{\mathbf{x}}_2, t)\mathbf{w}(t) + \mathbf{D}_2(\bar{\mathbf{x}}_2, t),$$
$$\mathbf{y} = \mathbf{x}_1, \qquad (51)$$

where

$$\mathbf{x}_1 = [x_{11}, x_{12}]^T, \quad \mathbf{x}_2 = [x_{21}, x_{22}]^T, \quad \boldsymbol{\theta}_1 = [0.5, 0.5]^T, \quad \boldsymbol{\theta}_2 = [1, 2]^T,$$

$$\mathbf{F}_1(\bar{\mathbf{x}}_1, t) = \begin{bmatrix} x_{11}e^{-0.5x_{11}} & 0 \\ 0 & x_{11}x_{12} \end{bmatrix},$$
$$\mathbf{F}_2(\bar{\mathbf{x}}_2, t) = \begin{bmatrix} x_{11}x_{21} & 0 \\ 0 & x_{11}x_{12}x_{22} \end{bmatrix},$$
$$\mathbf{G}_1(\bar{\mathbf{x}}_1, t) = \begin{bmatrix} 1 + \sin(x_{11}^2) & -2 \\ 5 & 2 + \sin x_{11} \end{bmatrix},$$
$$\mathbf{G}_2(\bar{\mathbf{x}}_2, t) = \begin{bmatrix} 3 + \cos(x_{21}x_{11}) & 0 \\ \cos(x_{22}) & 2 + \cos x_{12} \end{bmatrix},$$
$$\mathbf{D}_1(\bar{\mathbf{x}}_1, t) = \begin{bmatrix} 0.15\sin t + 0.35\sin(x_{11}x_{12}) \\ 0.6\sin x_{12} + 0.4\sin(2x_{12}t) \end{bmatrix},$$
$$\mathbf{D}_2(\bar{\mathbf{x}}_2, t) = \begin{bmatrix} 0.2\cos\left(x_{12} + x_{22}^2\right) + 0.3\sin(x_{11}t) \\ 0.4\cos(x_{21}) + 0.1\sin(0.5t) \end{bmatrix},$$

$$w(t) = [w_1(t), w_2(t)]^T = \begin{bmatrix} p_0 u_1(t) - \int_0^R p(r)F_r[u_1(t)]\,dr \\ p_0 u_2(t) - \int_0^R p(r)F_r[u_2(t)]\,dr \end{bmatrix}$$

with $p(r) = 0.5e^{-0.067(r-1)^2}$ and $R = 50$.

$\mathbf{F}_1(\bar{\mathbf{x}}_1, t)$ and $\mathbf{F}_2(\bar{\mathbf{x}}_2, t)$ are nonlinear system functions, and $\boldsymbol{\theta}_1$ and $\boldsymbol{\theta}_2$ are unknown system parameters, while $\mathbf{D}_1(\bar{\mathbf{x}}_1, t)$ and $\mathbf{D}_2(\bar{\mathbf{x}}_2, t)$ represent the system uncertainties. The control objective is to design robust control for system (51) such that the output of the system $\mathbf{y} = \mathbf{x}_1$ follows the desired output $\mathbf{y}_d = [0.5\sin t + \sin 0.5t, 0.8\cos 2t + 1.2\sin 0.2t]^T$.

Controller $\mathbf{u} = [u_1, u_2]^T$ is determined according to Theorem 1. The initial conditions and control parameters in this simulation are chosen as: $k_1 = 40$, $k_2 = 4$, $\rho_1 = \rho_2 = \lambda_1 = \lambda_2 = \kappa = \sigma = 2$, $\tau_1 = \tau_2 = 0.01$, $\varepsilon = 0.01$, $\mathbf{x}_1(0) = [0.1, 0.2]^T$, $\mathbf{x}_2(0) = [0.30.4]^T$, $\hat{\boldsymbol{\theta}}_1(0) = \hat{\boldsymbol{\theta}}_2(0) = \hat{\boldsymbol{\Xi}}_1(0) = \hat{\boldsymbol{\Xi}}_2(0) = [1, 1]^T$, and choose the level of discretisation $N = 500$ and $\hat{p}(i\Delta r) = 1$, for $i = 0{:}N$. In implementation, in order to avoid the chattering of the control input, the sign function sgn($\cdot$) is replaced with the saturation functionsat(S_{ni}/ξ), where $\xi = 0.01$.

The simulation results of the output tracking are shown in Figures 2 and 3, while the tracking error is presented in Figures 4 and 5, where we also compare it with the result without the hysteretic compensator for the nonlinearity of P-I hysteresis $\mathbf{u}_{HC}$. It is seen that with the proposed control scheme the output can follow the desired trajectories quickly within a very small error radius, despite the unknown bounded external disturbances, system parameters and hysteretic nonlinearity; and without the hysteretic compensator $\mathbf{u}_{HC}$, the tracking performance is much worse and the tracking error is much larger than that with the hysteretic compensator. Figures 6 and 7 show the controller input $\mathbf{u}(t)$ and the output of actuators with P-I hysteresis $\mathbf{w}(t)$, both of which keep bounded as time goes. It can be noted there exists obvious difference be-

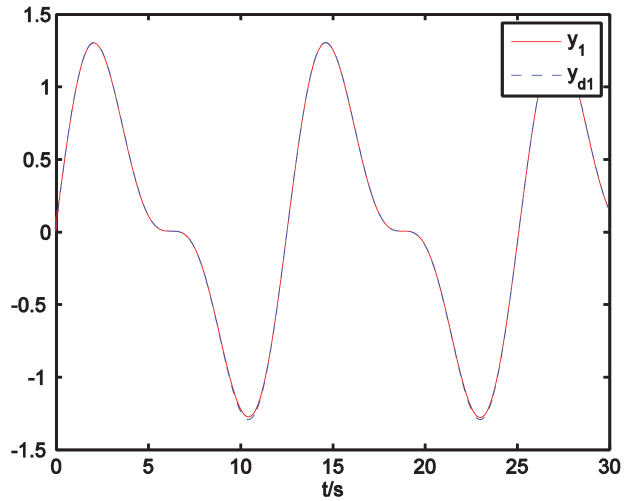

Figure 2. The trajectory of the output y_1 (solid line) and its desired trajectory y_{d1} (dashed line).

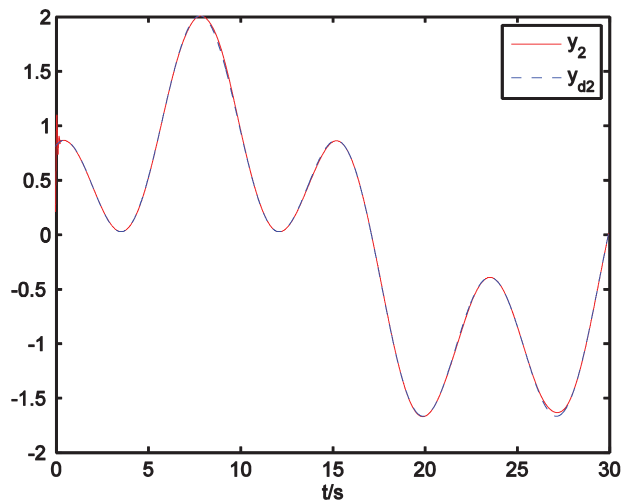

Figure 3. The trajectory of the output y_2 (solid line) and its desired trajectory y_{d2} (dashed line).

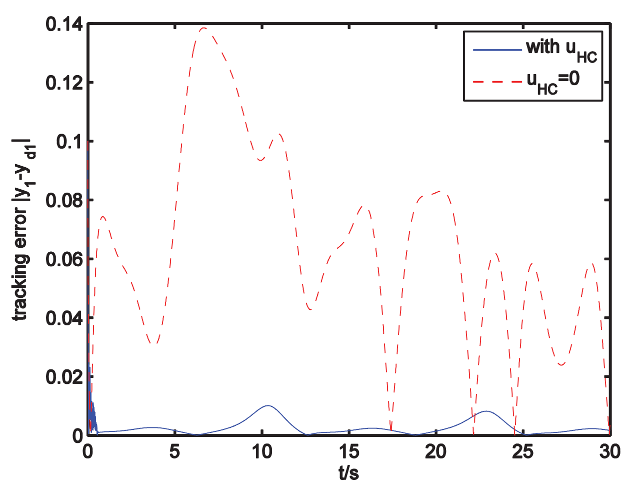

Figure 4. Tracking error between y_1 and y_{d1} with and without the hysteretic compensator $\mathbf{u}_{HC}$.

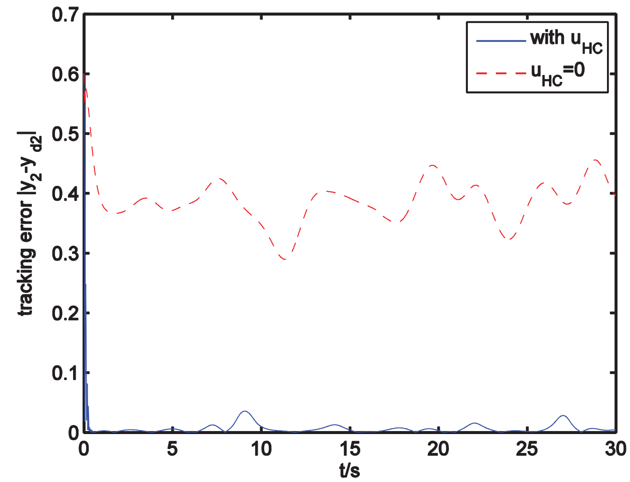

Figure 5. Tracking error between y_2 and y_{d2} with and without the hysteretic compensator $\mathbf{u}_{HC}$.

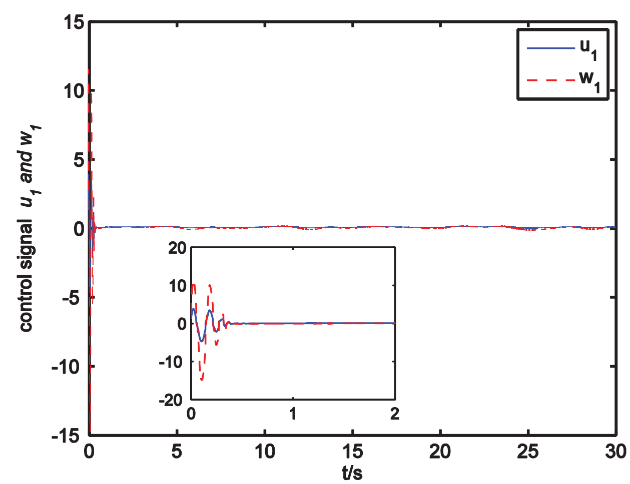

Figure 6. The control signal of u_1 and the output of the hysteretic actuator w_1.

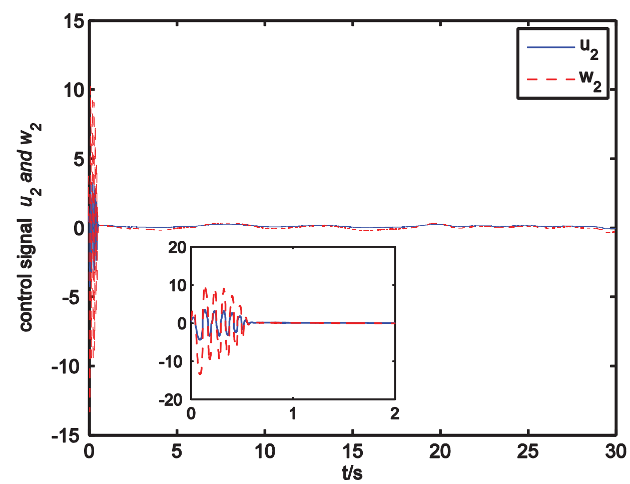

Figure 7. The control signal of u_2 and the output of the hysteretic actuator w_2.

tween the signals $\mathbf{u}(t)$ and $\mathbf{w}(t)$, which indicates the significant effect of the P-I hysteresis described by (4). It is indicated from these simulations results that under the controlled scheme (27), good tracking performance can be achieved.

5. Conclusion

In this paper, an adaptive robust control scheme is proposed for a class of nonlinear MIMO systems preceded by unknown P-I hysteresis based on the adaptive control and DSC. It is shown that under the proposed controller, the outputs of the controlled system can follow the desired trajectories with arbitrarily small tracking errors. The theoretical analysis is deduced based on Lyapunov synthesis and it is proved that all the signals of the closed-loop controlled system are ultimately bounded. Numerical simulations have been provided to illustrate the effectiveness of the proposed control scheme. The proposed scheme can be applied to a larger number of the nonlinear MIMO systems with either backlash hysteresis or such integral form as P-I hysteresis and the explosion of complexity caused by tedious computation of the time derivatives of the virtual control is overcome by introducing a low-pass filter. However, the effect of the saturation is not considered in this paper, while most of the actuators suffer from such nonlinearity in the real world application. Thus, it would be our future work to generalise the proposed control scheme to the system with saturation.

Acknowledgements

The authors are also thankful to the anonymous referees for their helpful comments.

Funding

This paper is partly supported by the National Science Foundation of China [grant number 61025016], [grant number 61473183], [grant number 61034008], [grant number 61221003], [grant number 61273116]; Program of Shanghai Subject Chief Scientist [grant number 14XD1402400]; SJTU M&E Joint Research Foundation [grant number YG2013MS04].

Notes on contributors

Guiyuan Fu is currently a PhD candidate in control theory and control engineering with Department of Automation, Shanghai Jiaotong University. He received his B.S. degree and M.S. degree in 2007 and 2010, respectively. His research interests include robust control of nonlinear system, complex system, opinion dynamics based on agent system.

Linlin Ou received her PhD degree in control theory and control engineering from Department of Automation, Shanghai Jiaotong University, China in 2006. She is currently a professor at the College of Information Engineering, Zhejiang University of Technology. Her research interests focus on theoretical aspects of time-delayed control systems, robot control, multi-agent system and cooperative control.

Weidong Zhang received his BS, MS and Ph.D. degrees from Zhejiang University, Hangzhou, China, in 1990, 1993 and 1996, respectively. He worked with the National Key Laboratory of Industrial Control Technology as a post-doctor before joining Shanghai Jiao Tong University, Shanghai, China, in 1998 as an associate professor. Since 1999, he has been a professor at the Department of Automation, Shanghai Jiao Tong University. He served as the deputy dean of the Department of Automation, Shanghai Jiao Tong University. He has authored or co-authored over 200 journal and conference papers. His research interests include robust control, distributed control and their applications in industry.

References

Anderson, M., Buehner, M., Yong, P., Hittle, D., Anderson, C., Tu, J., & Hodgson, D. (2008). MIMO robust control of HAVC systems. *IEEE Transactions on Control Systems Technology, 16*(3), 475–483.

Brokate, M., & Sprekels, J. (1996). *Hysteresis and phase transitions*. New York, NY: Springer-Verlag.

Cai, J., Wen, C., Su, H., & Liu, Z. (2013). Robust adaptive failure compensation of hysteretic actuators for a class of uncertain nonlinear systems. *IEEE Transactions on Automatic Control, 58*(9), 2388–2394.

Chen, M., Ge, S.S., & Ee, B.V. (2010). Robust adaptive neural network control for a class of uncertain MIMO nonlinear system with input nonlinearities. *IEEE Transactions on Neural Networks, 21*(5), 796–812.

Dawson, D.M., Carroll, J.J., & Schneider, M. (1994). Integrator backstepping control of brush DC motor turning a robotic load. *IEEE Transactions on Control Systems Technology, 2*(3), 233–244.

Deng, M., & Wang, A. (2012). Robust non-linear control design to an ionic polymer metal composite with hysteresis using operator-based approach. *IET Control Theory and Applications, 6*(17), 2667–2675.

Esbrook, A., Tan, X., & Khalil, H.K. (2013). Control of systems with hysteresis via servocompensation and its application to nanopositioning. *IEEE Transactions on Control Systems Technology, 21*(3), 725–738.

Gu, G.Y., Zhu, L.M., & Su, C.Y. (2014). Modeling and compensation of asymmetric hysteresis nonlinearity for piezoceramic actuators with a modified Prandtl–Ishlinskii model. *IEEE Transactions on Industrial Electronics, 61*(3), 1583–1595.

Jain, R.K., Majumder, S., & Dutta, A. (2012). Microassembly by an IPMC-based flexible 4-bar mechanism. *Smart Materials and Structures, 21*, 075004.

Kim, B., Ryu, J., Jeong, Y., Tak, Y., Kim, B., & Park, J.O. (2003). A ciliary based 8-legged walking micro robot using cast IPMC actuators. In: *Proceedings of ICRA'03 IEEE International Conference on Robotics and Automation* (pp. 2940–2945). Taipei, Taiwan: IEEE.

Krejci, P., & Kuhnen, K. (2001). Inverse control of systems with hysteresis and creep. *IEE Proceedings – Control Theory and Applications,* 148(3), 185–192.

Li, Y., Tong, S., & Li, T. (2012). Adaptive fuzzy output feedback control of MIMO nonlinear uncertain systems with time-varying delays and unknown backlash-like hysteresis. *Neurocomputing, 93*, 56–66.

Macki, J.W., Nistri, P., & Zecca, P. (1993). Mathematical models for hysteresis. *SIAM Review, 35*(1), 94–123.

Mousavi, S.H., Ranjbar-Sahraei, B., & Noroozi, N. (2012). Output feedback controller for hysteretic time-delayed MIMO nonlinear systems: An H^{∞}-based indirect adaptive interval type-2 fuzzy approach. *Nonlinear Dynamics, 68*, 63–76.

Parlangeli, G., & Corradini, M.L. (2005). Ouput zeroing of MIMO plants in the presence of actuator and sensor uncertain hysteresis nonlinearities. *IEEE Transactions on Automatic Control, 50*(9), 1403–1407.

Polycarpou, M.M., & Ioannou, P.A. (1996). A robust adaptive nonlinear control design. *Automatica, 32*(3), 423–427.

Qiao, J., Dai, Y., Liu, J., & Wang, H. (2007). Robust adaptive fuzzy output tracking control of uncertain robot system using backstepping design. *Proceedings of 26th Chinese Control Conference* (pp. 303–308). Zhangjiajie, China: IEEE.

Ren, B., San, P.P., Ge, S.S., & Lee, T.H. (2009). Adaptive dynamic surface control for a class of strict-feedback nonlinear systems with unknown backlash-like hysteresis. *Proceedings of American Control Conference* (pp. 4482–4487). St. Louis, Missouri: IEEE

Shan, Y., & Leang, K.K. (2009). Repetitive control with Prandtl-Ishlinskii hysteresis inverse for piezo-based nanopositioning. *Proceedings of American Control Conference* (pp. 301–306). St. Louis, Missouri: IEEE.

Su, C.Y., Wang, Q., Chen, X., & Rakheja, S. (2005). Adaptive variable structure control of a class of nonlinear systems with unknown Prandtl-Ishlinskii hysteresis. *IEEE Transactions on Automatic Control, 50*(12), 2069–2074.

Swaroop, D., Hedrick, J.K., Yip, P.P., & Gerdes, J.C. (2000). Dynamic surface control for a class of nonlinear systems. *IEEE Transactions on Automatic Control, 45*(10), 1893–1899.

Tan, X., & Baras, J.S. (2004). Modeling and control of hysteresis in magnetostrictive actuators. *Automatica, 40*(9), 1469–1480.

Tang, X.D., Tao, G., & Joshi, S.M. (2007). Adaptive actuator failure compensation for nonlinear MIMO systems with an aircraft control application. *Automatica, 43*(11), 1869–1883.

Tao, G., & Kokotovic, P.V. (1995). Adaptive control of plants with unknown hysteresis. *IEEE Transactions on Automatic Control, 40*, 200–212.

Vo-Minh, T., Tjahjowidodoand, T., Ramon, H., & Van Brussel, H. (2011). A new approach to modeling hysteresis in a pneumatic artificial muscle using the Maxwell-slip model. *IEEE/ASME Transactions on Mechatronics, 16*(1), 177–186.

Zhang, T.P., & Ge, S.S. (2007). Adaptive neural control of MIMO nonlinear state time-varying delay systems with unknown dead-zones and gain signs. *Automatica, 43*, 1021–1033.

Zhang, X., Lin, Y., & Mao, J. (2011). A robust adaptive dynamic surface control for a class of nonlinear systems with unknown Prandtl-Ishlinskii hysteresis. *International Journal of Robust and Nonlinear Control, 21*, 1541–1561.

Zhou, J., Wen, C., & Li, T. (2012). Adaptive output feedback control of uncertain nonlinear systems with hysteresis nonlinearity. *IEEE Transactions on Automatic Control, 57*(10), 2627–2633.